IEEE Access
Multidisciplinary ⋮ Rapid Review ⋮ Open Access Journal

Received 15 August 2023, accepted 11 September 2023, date of publication 19 September 2023,
date of current version 27 September 2023.

Digital Object Identifier 10.1109/ACCESS.2023.3317269

RESEARCH ARTICLE

Signaling Design for Cooperative Resource Allocation and Its Impact to Message Reliability

RASMUS LIBORIUS BRUUN[1], C. SANTIAGO MOREJÓN GARCÍA[1], TROELS B. SØRENSEN[1], NUNO K. PRATAS[2], TATIANA KOZLOVA MADSEN[1], AND PREBEN MOGENSEN[1,2]

[1]Wireless Communication Networks Section, Department of Electronic Systems, Aalborg University, 9220 Aalborg, Denmark
[2]Nokia Standardization, 9220 Aalborg, Denmark

Corresponding author: Rasmus Liborius Bruun (rlb@es.aau.dk)

ABSTRACT Decentralized cooperative resource allocation schemes for robotic swarms are essential to enable high reliability in high throughput data message exchanges. These cooperative schemes require control signaling to avoid half-duplex problems at the receiver and mitigate interference. We propose two cooperative resource allocation schemes, device sequential and group scheduling, and introduce a control signaling design. We observe that failure in the reception of these control signals leads to non-cooperative behavior and to significant performance degradation. The cause of these failures is identified, and specific countermeasures are proposed and evaluated through extensive system level simulations. The key performance indicators are data message reliability and the packet inter-reception metric. As our main reference, we compare the proposed resource allocation schemes against the NR sidelink mode 2 resource allocation, and show that despite signaling has a significant impact on resource allocation performance, our proposed device sequential and group scheduling resource allocation schemes improve reliability by an order of magnitude compared to sidelink mode 2.

INDEX TERMS Cooperative communication, distributed resource allocation, signaling, swarm communication.

I. INTRODUCTION

In today's society, it is insufficient to have connectivity only on smartphones. Wireless connectivity is expanding to wearables, domotics, automotive, etc., with the intent to make our lives simpler, safer, and more convenient. As connectivity becomes omnipresent, the basis for a new form of collaboration between connected devices has emerged. Nature has inspired many technological leaps, and the collaboration of simple entities is a well-known phenomenon in the animal kingdom. Here, ants, birds, bees, fish, and a plethora of other species have learned to benefit from collaboration allowing them to unite efforts and achieve complex tasks. The behavior of swarming, flocking, and schooling serves as inspiration for the collaboration which has become possible between connected electronic devices. The first use cases have already been envisioned, e.g.:

- In manufacturing, swarms are envisioned to enhance production lines by improved flexibility and adaptability enabled by better communication [1].
- In search and rescue flocks, drones are envisioned to cover land quickly and with short response time, thus vastly cutting the critical time to search for lost individuals in the debree of a collapsed building, people lost at sea, in a forest, etc. In such operations, it is vital to locate the missing individuals as soon as possible [2].
- Within the agricultural industry, in [3], a monitoring and mapping system guides autonomous weeding robots. This system maps and patrols the field using a UAV swarm. The system provides weed presence identification and the location of different intervention urgency areas.
- In domotics (smart home and office), the collection of connected smart devices (each with distinct sensing, actuating, or service functions) will collaborate to monitor the state of the building efficiently as the bee swarm maintains the hive. It provides an optimal indoor

The associate editor coordinating the review of this manuscript and approving it for publication was Fang Yang.

environment while minimizing the energy bill cost [4], [5]. The robot vacuum will operate where needed. However, it will do so at the most convenient times. Moreover, the heating, ventilation, and air-conditioning (HVAC) will be adjusted ad-hoc to provide the ideal indoor climate at all times [5], [6].

- In automotive, connected devices will be vital to maintain a streamlined transportation infrastructure, where the transportation needs of humans and goods can be met most safely and seamlessly possible. The sensors around the transportation grid will provide real-time traffic updates to the active vehicles, which will negotiate their optimal routes as they drive in dense platoons, not unlike ants and migrating birds [7], [8].

Undoubtedly, the most revolutionary applications of swarm robotics have yet to be discovered as technologies mature and become more accessible. Common for the previous use cases and the nature of swarms is the need for communication between devices within proximity. In theory, direct one-hop communication between devices has the shortest possible latency and the best utilization of time-frequency resources. Furthermore, it also provides suitable conditions for high reliability, which we define as the probability that a receiver successfully receives a message within an application's latency requirement. However, achieving these benefits will require more innovative solutions. Therefore, our efforts are concentrated on decentralized communication where all devices communicate on equal terms. Here, no coordination from the network or one specific device is needed for communication. Additionally, we are concerned with pushing beyond the current state of the art, thus focusing on how to improve throughput and reliability at reduced latency.

A. DECENTRALIZED WIRELESS COMMUNICATION

Different solutions exist for decentralized wireless communications; however, standardization is indispensable to achieve adoption and widespread usage. Standardized wireless communication technologies enable different manufacturers to produce compatible products. This aids competition and will produce a larger supply of products at a lower cost. The Institute of Electrical and Electronics Engineers (IEEE), Bluetooth Special Interest Group (SIG), and 3rd Generation Partnership Project (3GPP) govern the most known standards.

Bluetooth SIG governs the Bluetooth standard, a personal area network technology. Bluetooth Classic refers to the original Bluetooth protocol stack, originally meant as a wireless alternative to a cabled connection, e.g., between a headset and a phone. In version 4.0 of the Bluetooth Core Specification, the Bluetooth Low Energy protocol stack was introduced. Bluetooth Low Energy is incompatible with Bluetooth Classic and is designed for low power consumption. Both Bluetooth stacks operate in the unlicensed 2.4 GHz Industrial, Scientific, and Medical (ISM) band. The Bluetooth Mesh specification [9] was adopted in 2017 to allow Bluetooth technology to cater to applications that include multiple device networks.

The IEEE 802.15.4 standard is a low-data-rate, low-cost, and low-power physical and MAC layer specification [10]. It was initially conceived to enable low-cost personal area networks between ad-hoc devices and operates in the ISM bands between 0.8 and 2.4 GHz. IEEE also governs the 802.11 standards, a specification of protocols for wireless local area networks. The amendments 802.11a/b/g/n/ac/ax refer to WiFi networks, which connect computers and smartphones to the internet via an access point. However, 802.11s, 802.11p, and 802.11bd are amendments directed at device-to-device applications. The 802.11s amendment enables mesh networking in which packets are routed according to one of the supported protocols. Dedicated short-range communication is supported by the 802.11p and the upcoming 802.11bd amendments. These amendments aim to enable vehicular communication in the 5.9 GHz Intelligent Transport Systems (ITS) band.

The main challenge that Bluetooth SIG and IEEE governed standards have, is their operation in the unlicensed spectrum bands where they need to abide by either listen before talk or duty cycle restrictions [11], [12]. For this reason, these standards are vulnerable to interference and low spectral efficiency, which limits their achievable throughput and latency performance [13].

In the United States, the 3.5 GHz Citizen Broadband Radio Service (CBRS) band with a bandwidth of 150 MHz was established in 2015 to allow shared commercial usage in the band [14]. Up to 70 MHz is licensed by census tract (limited geographical region), allowing factories, airports, and the like to license the band and utilize it for a dedicated network. This licensing arrangement is interesting for future use cases of, e.g., cellular technologies, which already operate in this band in other parts of the world.

3GPP standardizes cellular communication. The concept of device-to-device communications appeared within 3GPP release 12, with the development of proximity services (ProSe). The most recent version of the standard is release 17. Among other things, it includes decentralized communications between user equipment (UE) in the form of New Radio (NR) sidelink resource allocation mode 2 (mode 2) with inter-UE coordination capabilities [15]. The mode 2 resource allocation is explained in detail in Section II-A. The presence of half-duplex problems and multi-user interference cause the main performance constraints of mode 2 [16]. Half-duplex is the limitation of the transceiver that it cannot simultaneously receive and transmit. The issue arises when two communicating transceivers transmit to each other simultaneously, rendering both unable to receive. Half-duplex and hidden terminals would cause imperfect sensing ending up in consecutive loss of status messages from neighbor devices [17].

Another issue in mode 2 is the effect of mismatch between the packet generation at higher layers and the periodical structure of resources at the lower layers that might reduce

performance [18]. The availability of empirical models for realistic generation of data could provide an accurate performance evaluation. In [19], authors proposed a set of models to realistically generate Cooperative Awareness Messages (CAMs) in vehicular networks.

Inter-UE coordination is an adopted option to mitigate half-duplex and interference problems. Two coordination schemes are agreed upon: Inter-UE coordination schemes 1 and 2. In scheme 1, upon request, the receiving UE-A assists the transmitting UE-B in resource allocation. It indicates a set of preferred/non-preferred resources for the transmitting UE-B; scheme 2 allows the receiving UE-A to notify the transmitter that the resource selected by the transmitter results in expected/potential and/or detected conflicts.

The inter-UE coordination framework introduced in 3GPP Rel.17 does not target swarm use cases where a group of UEs has to exchange information. In other words, the signaling is pair-based and inefficient for use cases where a group of UEs requires coordination information.

B. COOPERATIVE COMMUNICATIONS

Consensus on the use of time-frequency resources is the basis of multi-user communication. In decentralized communication systems, one way to achieve high throughput, high reliability, and low latency is to reach consensus in the usage of time-frequency resources via cooperative resource allocation. Authors in [20] introduce two consensus communication protocols, the first being a gossip-based (multi-hop message diffusion) and the second a broadcast (single-hop message diffusion) communication protocol. In both protocols, a set of UEs (validators) validate and commit the proposed action (vacant frequency band) made by the proposer UE. The consensus protocols have low latency and high reliability that could support mission-critical and real-time tasks, as long as consensus decisions change infrequently. The validation process may take some time, due to the number of validators, and conversely if this number reduces, reliability may suffer. Therefore, there is a need for a balance between reliability and latency. The main advantage of the consensus algorithm is its resilience to UEs with malicious intent.

In systems without ''malicious UEs'', the consensus procedure is no longer necessary since it is assumed that all nodes will follow the specified resource allocation procedure. Consequently, an optimal resource allocation scheme can be reached faster. Authors in [21] develop resource allocation algorithms inspired by bio-swarming behavior. The presented methods rely on multiple iterations before they converge to an optimal resource allocation. In [22] the authors present a distributed resource allocation scheme which converges in quadratic time. The convergence is dependent on the number of devices, as each device is involved in the execution of the algorithm.

Although these distributed consensus and resource allocation schemes achieve full alignment of the swarm members and an optimal resource allocation, the involvement of the majority of the swarm members in the allocation process is detrimental to the latency as the swarm size grows. Instead, it is desired that changes to the resource allocation can be performed locally among one or several sub-sets of swarm members, in such way that overhead in the form of control signals is limited. Fig. 1 illustrates three methods for resource allocation (RA) control signaling, where 2 adjacent frequency separated resource pools exist; one for dedicated control signals and one for data messages. Mode 2 employs resource allocation control signaling method 1, where control signals are embedded with the data messages and thus only reach nearby swarm members (a more detailed explanation of mode 2 operation is provided in Section II-A).

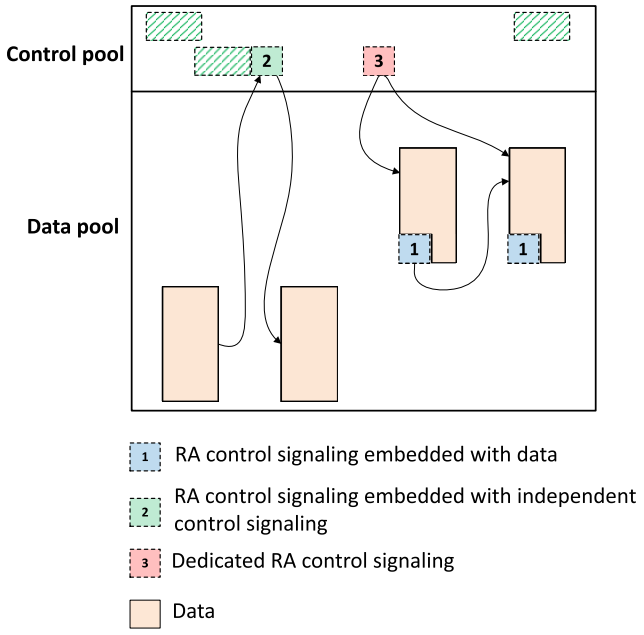

FIGURE 1. Methods to exchange signaling: 1) Embedded with data (blue), 2) Embedded with independent signaling (green), and 3) Dedicated (red).

In recent literature, cooperative extensions to the existing NR mode 2 standard have been suggested in an effort to address shortcomings in the current version. The continuous collision issue of the semi-persistently scheduled (SPS) transmissions is tackled in [23] by allowing a third UE to piggyback with its own transmission an indication that continuous collision is (likely) taking place in another resource (method 1 in Fig. 1). It is a reactive scheme where collisions are resolved rather than avoided. The scheme depends on other UEs being able to assist. In [24] authors introduce a counter in the SPS signaling indicating the time of reselection, i.e. as method 1 in Fig. 1. Within each SPS transmission, a procedure is proposed to adjust the counters such that no UE will be reselecting in the same transmission time interval, thus mitigating SPS collisions. The procedure is proactive as it tries to mitigate future collisions, however, the procedure is designed for low density swarms. Additionally, failures on the initial transmission are not handled. The

piggybacking of control signals to periodic safety messages in [25] indicates the future resource allocation of SPS transmissions (method 2 in Fig. 1). The next SPS allocation is performed before the end of the current SPS transmission, allowing time to reselect the SPS in case of potential conflict.

To address the mode 2 limitations (i.e., susceptibility to half-duplex and interference), in our previous work, we introduced two cooperative resource allocation schemes, device sequential and group scheduling. They have different resource allocation algorithms and cooperation schemes, however, follow the 3GPP sidelink mode 2 framework [26]. Both schemes allow coordination where message exchange is only required for devices in proximity with an immediate need for communication resources. The additional signaling required could partly be piggybacked to existing discovery messages (method 2 in Fig. 1) and by the introduction of a dedicated control signal (method 3 in Fig. 1). Under the assumption of perfect exchange of control signals, the proposed schemes outperformed mode 2 [26].

C. OUR CONTRIBUTION

In this article, we recapitulate the device sequential and group scheduling resource allocation schemes, and additionally design the required signaling exchange to evaluate its impact on data message reliability. We show how device sequential and group scheduling schemes provide significant performance improvement over the baseline, despite introducing signaling overhead. Our evaluation focuses on the causes of data message failures, thereby allowing a deeper analysis of the signaling design, its impact on the resource allocation, and the resulting data message performance. Additionally, it provides us information to propose techniques to overcome such failures, and evaluate their impact on the final data message reliability. The specific contributions in this article are:

- Specific signaling design to enable distributed cooperation for the proposed device sequential and group scheduling cooperative resource allocation schemes.
- Monte Carlo evaluation of the impact of the signaling design on the performance of the proposed schemes, in comparison to the standardized NR sidelink mode 2 with signaling.
- A methodology of analysis for separating communication failures and identifying the most impacting causes, thereby deepening the understanding of performance differences and focal points for further enhancements.
- Techniques to enhance the signaling reliability and overall swarm application performance for the two proposed resource allocation schemes, based on the specific causes of failure.

The communication requirements addressed in our work exceeds that of related literature by an order of magnitude. Specifically, we consider throughput, latency, and reliability requirements of 10 Mbps, 10 ms, and 99.99 %, respectively. For example, in [19], authors consider that vehicles transmit collision avoidance messages (CAMs) whose size does not surpass some hundreds of bytes and, when transmitted at most every 100 ms, equates to a throughput in the order of tens of kbps. The considered latency is hundreds of milliseconds, far from our assumed 10 ms maximum latency. The cooperative schemes we analyze, improve and design signaling for, retain a high degree of configurability. This is important to cater for high performance applications, as illustrated by the authors of [18]. They show that inability to accommodate potential misalignment between application layer data generation and the resource allocation can be detrimental to the performance of the application.

We continue with Section II presenting the assumptions, notation, and the baseline mode 2 allocation scheme. In Section III, we present the cooperative resource allocation schemes device sequential and group scheduling. Control signaling design for the cooperative schemes are presented in Section IV. Section V outlines the simulation setup and the simulation results and enhancement techniques are presented and evaluated in Section VI. Concluding remarks are made in Section VII.

II. SYSTEM MODEL AND NOTATION

Consider a system of N UEs engaging in proximity communication, enabled by their omnidirectional antennas and half-duplex radios. At any point in time, a UE is either not involved in proximity communication, and therefore not transmitting data messages, or the UE is involved in proximity communication. Proximity communication takes place between UEs within (a device-centric) critical communication range of r_c. We differentiate between *data messages*, defined as the information bits transmitted for the purpose of some swarm application, and *control signals*, defined as the transmitted bits, which serve a supporting function not directly related to the swarm application. UEs determine their own position and share it as part of the control signals. Therefore, only one position is associated with each UE. Inaccuracy in the positioning method will affect the perception of when UEs enter/depart the critical communication range. This inaccuracy has indirect effect on the process of the resource allocation, as the reliability of control signal and data message exchanges could suffer from increased path loss caused by UEs engaging in resource allocation at longer distances. In this work, we disregard the effect of positioning accuracy.

The proximity communication consists of transmitting and receiving multi-casted data messages of size x_d bytes with a d_p seconds periodicity to and from all UEs within proximity; i.e., a UE will transmit data at an average rate of $t_d = x_d/d_p$ bytes per second during proximity communication. The need to transmit data messages is determined based on proximity: the *ready time* is the moment in time when a data message is ready from the application layer. A maximum latency of l seconds can be tolerated from the ready time until the message is delivered to all intended destinations. Combined, the ready time and latency budget define the deadline of the data messages. The data message becomes useless after the

TABLE 1. Notation.

Symbol	Meaning
N	Total number of autonomous robots
W	Bandwidth for data message transmissions
S	Number of slots in the lifetime of the network
r_e	Extended cooperation range
r_c	Critical cooperation range
n_s	Number of slots requested by a UE for its transmission
$\mathcal{N}$	Set of UE IDs $\mathcal{N} = \{1, 2, ..., N\}$
$\mathcal{S}$	Set of time slots $\mathcal{S} = \{1, 2, ..., S\}$
$\mathcal{C}^{(s)}$	Set of candidate slots available to a UE for allocation of the data message generated in slot s
$\mathcal{R}_s$	Resource occupancy determined by sensing procedure
$\mathcal{R}_e$	Resource occupancy determined by exchange of control signals
$\mathcal{A}$	Slots allocated for requested transmission(s)
s	Indicates a unique slot in $\mathcal{S}$
o	Indication of the occupancy in a slot
d_p	Transmission periodicity
d_s	NR slot duration
x_d	Size of data message in bytes
t_d	Data message data rate
p_{tx}	Transmission power
T	Thermal noise power
$g^s_{n,n'}$	Channel gain between UEs n and n' in slot s
$\gamma^s_{n,n'}$	SINR on transmission between UEs n and n' in slot s

deadline and will be discarded. Some control signals might be exchanged regardless of proximity.

We follow the 3GPP system framework [27] where communication is based on Orthogonal Frequency Division Multiplexing (OFDM) on a frequency band of bandwidth B. The frequency resource is shared between UEs by time division multiple access (TDMA). The smallest allocation unit is called a slot and has duration d_s, which is configurable based on the selected numerology. For simplicity we adhere to numerology 2, the highest numerology available for frequency range 1, which results in the shortest slot duration. We refer to time slots by their index s in the set $\mathcal{S} = \{1, 2, \ldots, S\}$, which spans the lifetime of the network. For simplicity, we assume UEs to have the same transmission requirements and to be time synchronized, i.e. following the 5G NR procedure explained in [28]. In the following sections we use the notation in Table 1.

When a UE with id $n \in \mathcal{N} = \{1, 2, \ldots N\}$ generates data in a slot s, this data is associated with a group of receivers $\mathcal{N}' \subset \mathcal{N}$ where $n' \in \mathcal{N}' : n' \neq n, \text{dist}(n', n) < r_c$. The function $\text{dist}(n', n)$ returns the euclidean distance between UEs n' and n. For simplicity, we assume that every transmission is subject to the same transmission power p_{tx}. The channel gain on the transmission from n to n' in slot s is given as $g^s_{n,n'}$ and the gain on the interfering transmissions is given as $g^s_{k,n'}$ $\{k : k \in \mathcal{K} \subset \mathcal{N}, k \neq n, k \neq n'\}$. The channel gains are modeled as the combined effect of path loss and shadowing, where the shadowing component on different links is correlated.

When a slot is used for transmission, the SINR on a link between n and n' in slot s is calculated according to

$$\gamma^s_{n,n'} = \frac{p_{tx} g^s_{n,n'}}{T + \Sigma_{k \in \mathcal{K}} p_{tx} g^s_{k,n'}} \tag{1}$$

where T is the thermal noise power.

Based on the ready times and latency requirement, the three-dimensional latency matrix can be obtained $\mathbf{D}_{N \times N \times S} = [\delta_{n,n',s}]$. $\delta_{n,n',s}$ signifies the last possible slot in which data generated by n in slot s should be transmitted for n' to receive it within the latency constraint.

$$\delta_{n,n',s} = \begin{cases} s + \lfloor \frac{l}{d_s} \rfloor, & \text{if } n \text{ generates data in slot } s \text{ which should be transmitted to } n' \text{ within latency } l \\ 0, & \text{otherwise} \end{cases} \tag{2}$$

The problem is to determine an allocation, indicated by the allocation matrix $\mathbf{A}^*_{N \times S} = [\alpha_{n,s}]$ where the maximum number of UEs can be supported in the swarm.

$$\alpha_{n,s} = \begin{cases} 1, & \text{if } n \text{ transmits in slot } s \\ 0, & \text{otherwise} \end{cases} \tag{3}$$

For each nonzero entry $\delta_{n,n',s}$ in $\mathbf{D}$, the corresponding transmissions can be determined as the nonzero entries of $\mathbf{A}$ in the corresponding row n and the columns in the allocation interval $[s; s + \lfloor \frac{l}{d_s} \rfloor]$. The slots in the allocation interval constitute the candidate slot set $C^{(s)} = \{s, \ldots, s + \lfloor \frac{l}{d_s} \rfloor\} \subset \mathcal{S}$ a UE could possibly be allocated for transmission of the data message generated in slot s. Let $\Delta_{\delta_{n,n',s}} = \{\alpha_{n,r} : r \in S, s <= r <= s + \lfloor \frac{l}{d_s} \rfloor\}$ be the set of slots n utilized for the transmission of data to n'. The effective SINR of the transmissions relating to the same data message can be calculated as

$$\gamma_{\delta_{n,n',s}} = 2^{\frac{1}{K} \sum_{r \in \Delta_{\delta_{n,n',s}}} log_2(1 + \gamma^r_{n,n'})} - 1 \tag{4}$$

which is also known as the mean instantaneous capacity method used to determine an effective SINR mapping [29]. Thus, defining the set $\Gamma = \{\gamma_{\delta_{n,n',s}} : \delta_{n,n',s} \neq 0, n \in N, n' \in N', s \in S\}$ with cardinality $|\Gamma|$, the optimization problem can be formulated as

$$\mathbf{A}^*_{N \times S} = \arg\max_{\mathbf{A}_{N \times S}} \quad N \tag{5a}$$

$$\text{subject to} \quad \frac{1}{|\Gamma|} \Sigma_{\gamma_i \in \Gamma 5pt} \text{bler}(\gamma_i) < f_p, \tag{5b}$$

$$\forall n \in N : \alpha_{n,s} + \Sigma_{i \in N' 5pt} \alpha_{i,s} <= 1 \tag{5c}$$

where $\text{bler}(x)$ is a mapping function which maps a certain SINR to a block error rate, following the physical layer abstraction given in [30]. The first constraint (5b) guarantees that the average system failure probability does not exceed a required failure probability requirement, f_p. The second constraint (5c) ensures that no two UEs within critical cooperation range transmit simultaneously, thereby avoiding half-duplex problems.

The issue of determining the allocation matrix $\mathbf{A}$ (like the problem formulated in [31]) is NP-hard, thus no algorithm can be found to determine the optimal solution within polynomial time. Additionally, due to the potential overlap

of allocation intervals of different UEs, in search of the optimal solution, the entire lifetime of the network should be considered. Therefore, it is not feasible to find an exact solution to this problem, and instead we resort to heuristic methods in efficiently determining suboptimal solutions to the allocation problem in a decentralized manner. We note that these approaches limit the scope of each round of allocation such that only $\mathcal{C}^{(s)}$ is considered. Furthermore, due to the decentralization of the system, the allocation decision can be delegated to each UE, which might have a limited knowledge about the allocation decisions of other UEs. We will see that knowledge of other UEs allocation decisions is important for the performance of the system, as it might help avoid half-duplex allocations and reduce interference. In the next section, the state of the art decentralized resource allocation algorithm of 5G NR is presented.

A. BASELINE RESOURCE ALLOCATION SCHEME (MODE 2)

On the sidelink, UEs can transmit directly to each other by performing 5G NR sidelink resource allocation mode 2 [32]. Mode 2 relies on the signaling exchanged in the sidelink control information (SCI). The SCI is transmitted as part of a data message as depicted by control signal method 1 in Fig. 1. The SCI carries information which is necessary for the decoding of the data message, but more importantly (in a resource allocation perspective) it indicates the periodicity of the data message transmission, i.e. the future resources reserved for this semi-persistently scheduled (SPS) transmission. SPS transmissions introduce predictability, which allow other UEs to avoid allocation of conflicting resources. In addition, the UEs can reuse the resource allocation of one data message for subsequent data messages. This is a key concept of mode 2 by which UEs autonomously allocate resources. For completeness, we summarize the two stages of mode 2 below.

1) SENSING STAGE

Sensing is performed on a *sensing window*, which spans the bandwidth configured for mode 2 transmissions in frequency and a span no longer than 1 s in time leading up to the selection stage. The goal of the sensing is to determine a set of resource candidates. Initially, a set of resource candidates of size $|\mathcal{C}^{(s)}|$ is defined. Candidates are removed from the resource set if an SCI received during the sensing window indicates that the resource candidate is reserved by another UE and the measured reference signal received power (RSRP) on the SCI is above a threshold. If the resulting resource set is smaller than 20% of $|\mathcal{C}^{(s)}|$, the threshold is increased by 3 dB and the discarded resource candidates are re-evaluated, i.e. re-introduced to the resource set if the RSRP is below the threshold.

2) SELECTION STAGE

In the selection stage the resource allocation algorithm is performed. It consists of selecting the requested resource(s) randomly among the resource candidates. If the resources are reoccurring with a given periodicity, the SPS re-selection counter is initialized [33]. At each transmission using the allocated resource, the counter is decremented. Once the counter reaches zero, re-selection is performed according to the mode 2 resource allocation.

Algorithm 1 Resource Allocation

Input: $\{(n_s, \mathcal{R} = \{\mathcal{R}_s \cup \mathcal{R}_e\})_k\}, k = 1, 2, \ldots, K$
Algorithm:

```
for each k in descending order of number of UEs within critical cooperation range do
    P = {(s, o)_i ∈ R_k | o_i ≠ ∞}
    for n = 1, 2, ..., n_{s,k} do
        i* = arg min_i o_i ∈ P
        A_k ← A_k ∪ s_{i*}
        P ← P − (s, o)_{i*}
    end for
end for
```

Output: $\{\mathcal{A}\}_k$

The advantage of mode 2 is the autonomy of the procedure. It is only affected by the information it is able to obtain during the sensing window, and the delay introduced by determining the candidate slots is fixed. The disadvantage is that the simple coordination might cause two UEs with close ready times to independently allocate overlapping resources, resulting in half duplex problems. Additionally, the random nature of the allocation can cause sub-optimal performance.

In the following, we introduce our cooperative resource allocation schemes. Both were built to comply with the 3GPP sidelink framework and its possible extensions. The sidelink framework is different from the framework of ISM-band technologies, where listen-before-talk and duty cycle restrictions are essential bounds on the resource allocation. Therefore, mode 2 acts as the baseline to which we compare our proposed allocation schemes.

III. PROPOSED COOPERATIVE RESOURCE ALLOCATION SCHEMES

The cooperation scheme refers to the distribution of the resource allocation and related functions. It answers the question of who will perform the resource allocation, when, and based on what information. As in Fig. 1, we assume the bandwidth is divided into two adjacent frequency resource pools, to accommodate control signals and data messages respectively. The UEs are able to either transmit or receive in both resource pools simultaneously, but due to the half-duplex constraint, simultaneous reception and transmission is not possible. Section IV will explain which types of signals are transmitted in the control pool. The control pool signals are intended for UEs within an extended device centric communication range of r_e.

Both proposed resource allocation schemes described here share the same basic resource allocation algorithm

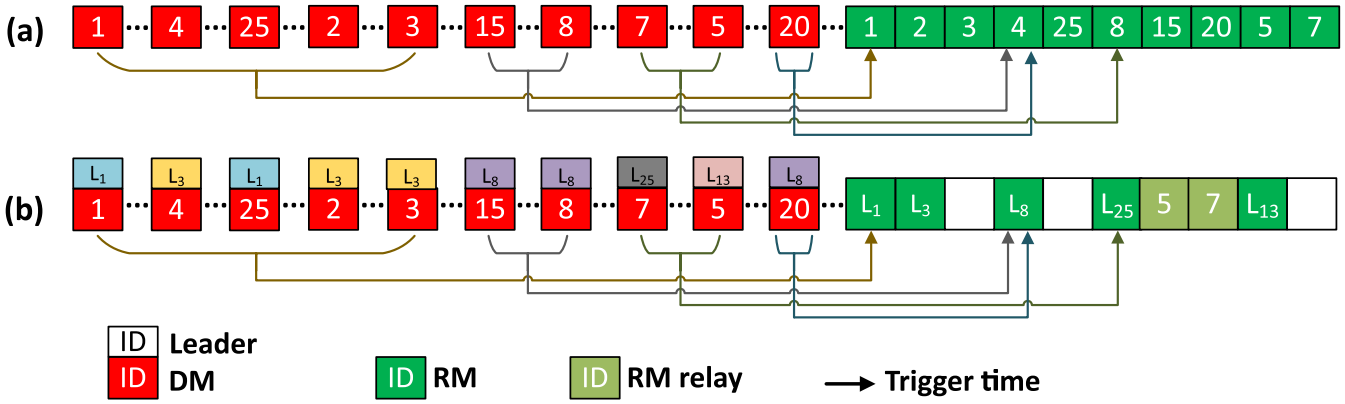

FIGURE 2. Relation between discovery messages (DMs) illustrated by red boxes and resource selection messages (RMs) illustrated by green boxes for (a) device sequential and (b) group scheduling schemes. ID is UE identification.

(Algorithm 1). We differentiate between the *allocating* UE, which is the UE executing the resource allocation algorithm, and the *requesting* UE(s)$^{1,\ldots,K}$, which is the UE(s) requesting an allocation from the allocating UE. The allocating and requesting UE can be the same UE. The input is the tuple $(n_s, \mathcal{R} = \{\mathcal{R}_s \cup \mathcal{R}_e\})_k$ for each user k where n_s is the number of slots requested by the requesting UE. The predictability of SPS transmissions will be utilized in the proposed schemes. A benefit of SPS transmission is that one resource allocation can be valid for multiple data message transmissions. Allocation of an SPS transmission is triggered at the *trigger time*. The trigger time occurs when the number of UEs within r_c is incremented to one (no longer zero) or after the resource re-selection counter expires. The resource re-selection counter is defined in [34] and decrements at each data message transmission. The UE can determine the trigger time either by estimating when another UE will be within r_c or when the re-selection counter reaches zero. The resource pool occupancy is given by the set $\{\mathcal{R}_s \cup \mathcal{R}_e\}_k = \{(s, o)_i | s_i \in \mathcal{C}_k^{(s)} \wedge o_i \in \mathbb{R}\}$ where o_i is an indication of the occupancy, defined as the strongest signal previously received from any of the UEs expected to transmit in slot s_i. If a slot s_i is occupied by a UE within critical cooperation range of the requesting UE, the corresponding o_i is set equal to infinity to avoid the half-duplex problem. Conversely, if no other UE transmits data in slot s_i, then o_i is set to negative infinity, thus $|\mathcal{C}_k^{(s)}| = |\mathcal{R}|$. $\mathcal{R}_e$ is provided by the allocating UE while n_s and R_s are provided by the requesting UE. R_s indicates the current resource utilization as observed by the requesting UE whereas $\mathcal{R}_e$ indicates the resource utilization obtained (through control signaling) by the allocating UE. If K UEs are requesting an allocation from the same allocating UE simultaneously, their inputs will be ordered according to their priority, with $k = 1$ indicating the highest priority UE and $k = K$ the lowest priority UE.

Based on the resource occupancy from the requesting UE(s) and the received control signals, the resource allocation algorithm (Algorithm 1) allocates the resources for UE^k, to avoid half-duplex problems and ensure the lowest interference from other UEs. If multiple requesting UEs are being assigned a resource allocation, the requesting UE with most potential half-duplex conflicts (most UEs in critical cooperation range) has resources allocated first. This greedy selection scheme is also known from greedy graph coloring algorithms. For each requesting UE, a set $\mathcal{P}$ of candidate resources is initialized based on the resource pool occupancy observed by UE^k. Resources are allocated based on the lowest occupancy in lines 4 and 5 of Algorithm 1. In case multiple slots have identical minimum occupation in line 4, one will be randomly selected. A slot is allocated for UE^k in line 5 and the corresponding entry is removed from set $\mathcal{P}$ in line 6. As a result, the output of the resource allocation algorithm is the set of allocated resources, $\mathcal{A}_k \subseteq \mathcal{C}_k^{(s)}$, for each of the requesting UEs.

A. DEVICE SEQUENTIAL RESOURCE ALLOCATION SCHEME

This scheme consists of coordinated resource selection by following a sequence in which UEs independently perform resource allocation in prioritized order. In our design, the UE priority is based on their trigger time and a unique ID. The UE with earliest trigger time has highest priority, and in case multiple UEs possess identical trigger time, the unique UE ID determines the sequence such that lower ID has a higher priority.

In Fig. 2 (a) the red boxes indicate the point in time when the trigger time is announced (in a discovery message discussed in Section IV-A). UEs 1, 4, 25, 2, and 3 have the same trigger time as indicated by the arrow pointing to the time slot for resource allocation. Due to the trigger time collision between the 5 UEs, UE 1, having the highest priority, performs its resource allocation at the trigger time and immediately transmits its resource allocation message. UEs 2, 3, 4 and 25 in turn and according to their priority awaits reception of the resource allocation message from the higher priority UE(s), then immediately perform resource allocation and transmit their resource allocation message. Thus, UEs 2, 3, 4, and 25 perform resource allocation after their indicated trigger times (respectively a delay of 1, 2,

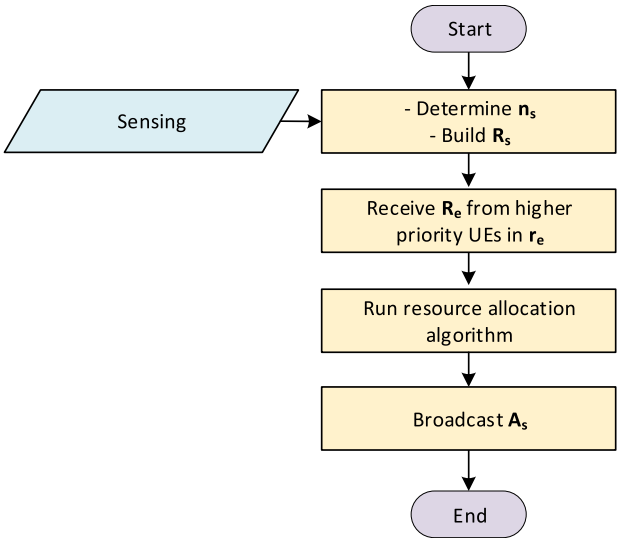

FIGURE 3. Device sequential coordination scheme for UE_i.

3, and 4 time slots). The coordination scheme for device sequential resource allocation follows the flow presented in Fig. 3. A UE continuously monitors the trigger time and position of other UEs within the extended cooperation range r_e. Once the UE requires resources, it initiates the resource allocation scheme. After determining the number of resources necessary for the transmission, the UE awaits the resource selection from higher priority UEs within r_c, and continues when either resource selection has been received from all higher priority UEs or the *resource selection delay* expires (further discussed in Section IV). The resource selection delay is a configurable parameter. Then, the UE executes the resource allocation algorithm, providing itself with a resource allocation. The allocated resources are signaled by broadcast intended for every other UE within r_e.

The advantage of the device sequential scheme is the autonomy with which each UE is performing its own resource allocation, while simultaneously coordinating with UEs in extended coorperation range. Additionally, the prioritization scheme, while important for the coordination, is also a way of providing differentiated service to the swarm member UEs. The potential drawback of the scheme is the risk of additional resource allocation delay. The delay is linear with the number of UEs within r_e which have overlapping trigger time. Thus, it is affected by the density of the swarm and the frequency of the resource re-selection, which is controlled by the resource re-selection counter.

B. GROUP SCHEDULING RESOURCE ALLOCATION SCHEME

As implied by the naming, the group scheduling resource allocation scheme relies on local groups, in which a group leader is executing the resource allocation algorithm and supplying the group members with resource allocation. Coordination happens within the group, but also between

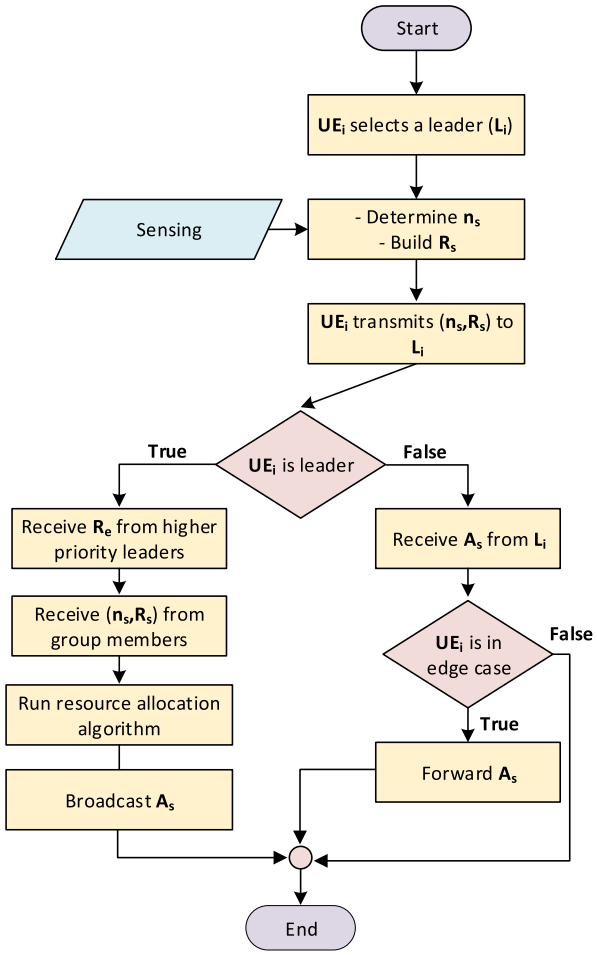

FIGURE 4. Group scheduling coordination scheme for UE_i.

groups. For the latter, group leaders are either within extended cooperation range of, or have group members which collaborate with UEs in another group. The group leader coordination is similar to the sequential scheme, where the prioritized order of allocation is determined by firstly, group member trigger time (earlier trigger time is higher priority) and secondly, the group leader unique ID (lower ID is higher priority). E.g, in Fig. 2 (b) UEs 1 and 3 have been elected as leaders with IDs L_1 and L_3, respectively. Both leaders have group members with the same trigger time (UEs 1 and 25 for L_1 and UEs 2, 3, and 4 for L_3). L_1 has highest priority, thus performs resource allocation for its group members before L_3. The flow of the group scheduling resource allocation scheme is presented in Fig. 4.

A UE continuously maintains membership of a group. It does so by periodically performing leader selection and broadcasting its choice of group leader. The candidate leaders are all UEs within r_e. Out of the candidate leaders, the leader is chosen as the candidate with most UEs within its r_c. The unique UE ID will resolve any ties, such that the candidate leader with the lowest ID UE will be selected as the leader. Thereby, the group leaders are bound to be

involved in swarm communication. Ahead of the trigger time, a UE informs its leader of its trigger time, the number of requested resources, the sensed resource occupation, and the candidate slots. At the trigger time, the leader executes the resource allocation algorithm after receiving any potential resource selection from higher priority leaders within r_e, or at latest when the resource selection delay has expired. The output from the resource allocation is signaled to the requesting UE and any lower priority leaders within r_e. Due to the range controlled leader selection procedure, the leaders of two collaborating UEs might be outside extended coordination range, potentially not being able to directly communicate. We refer to this as the *edge case*. In edge cases, the collaborating UEs need to forward the resource allocation received from their leader to allow the leaders to coordinate the resource allocation. Such forwarding is performed by UE 5 and 7 in Fig. 2.

The advantage of the group scheduling scheme is that leaders are able to perform resource allocation for multiple UEs simultaneously and combine their allocation in a single control message, thereby reducing the amount of messages used for control signaling. Additionally, the group leader has more information for resource occupation, as each group member and the group leader itself collects resource occupation information. The disadvantages relate to the additionally required control signals. The resource allocation must be signaled between leader and requesting UE. Failure to receive this signal will cause the requesting UE to be without a resource allocation. The requesting UE must provide information to the leader which incurs additional signaling overhead. Lastly, the edge case, where coordinating leaders are out of direct communication range, will cause a coordination delay and additional overhead.

IV. CONTROL SIGNALING FOR COOPERATIVE SCHEMES

The decentralized cooperative resource allocation schemes require additional control signaling exchanges compared to mode 2. In this section we establish the control messages which will carry the control signals. For the cooperative schemes we utilize all three methods in Fig. 1 (RA control signaling embedded with data, embedded with independent control signaling, and dedicated) for exchanging control signals. A summary of the control signals and their control information for each resource allocation scheme is presented in Table 2. The data message is identical for all schemes and simply include an indication of the periodicity of the message, making any receiver able to determine future resource reservation. The next subsections will elaborate on the discovery and resource selection message types.

A. DISCOVERY MESSAGE (DM)

The objective of DMs is for UEs to become aware of each others ID, position, and heading direction. It is transmitted periodically with no exceptions. The DM is necessary regardless whether the resource allocation scheme is cooperative or non-cooperative, e.g. mode 2. Each DM is scheduled randomly within the discovery period.

For the device sequential and the group scheduling schemes the DMs are extended with information about the **trigger time**, when this is known by the UE. We assume that the trigger time can be estimated far in advance and that the value of the reselection counter is randomly selected in the interval [25,75] as specified in [33] equating to at least 250 ms between resource reselection. A 100 ms discovery period would lead to each UE having at least 2 DM transmissions to successfully discover peers.

In the group scheduling scheme, the DM is extended with additional information. The leader selection is included in each discovery message such that leaders and collaborating UEs remain updated about the existing groups. When the trigger time approaches, the requesting UE will include the sensing result in its DM for the leader to use during resource allocation. Additionally, if UE-A identifies that its leader, L_A, and the leader, L_B, of a collaborating UE-B are out of direct communication range (the edge case scenario), UE-A will indicate in the DM (special forward indication) the ID of L_B and the trigger time of UE-B. This special forward indication allows L_A to determine the priority between the leaders and follow the coordination procedure. The size of DMs is enlarged by tenths of bytes due to the extensions needed by the cooperative schemes.

B. RESOURCE SELECTION MESSAGE (RM)

This control signal is exclusive to the cooperative resource allocation schemes. Its function is to carry information about the allocated resources for future data messages. Hence there is a direct connection between RM transmission and the trigger time indicated in the DMs. Compared to the non-cooperative scheme, the RM represents an additional overhead. However, it is transmitted only once per SPS period. Fig. 5 presents the RM transmission sequence diagram for each of the cooperative resource allocation schemes. The particularities of RMs for device sequential and group scheduling schemes are the following.

1) DEVICE SEQUENTIAL

At the trigger time a UE allocates resources and transmits its RM unless one of the two following conditions are true:

1) there are UEs with higher priority (lower unique ID) within r_e with the same trigger time (e.g. UE 3 waits for UE 2's RM in Fig. 5 (a)), or
2) there are UEs within r_e, with earlier trigger time, which are pending to perform resource allocation (e.g., UE 8 is waiting for UE 25's RM in Fig. 2 (a)).

Therefore, upon reception of RMs from higher priority UEs or when the predefined resource selection delay has expired, the UE will proceed to send its RM. Even though the delay to perform resource allocation scales linearly with the number of higher priority UEs in the sequence, it is bound by the resource selection delay. Resource allocation commences

TABLE 2. Message content necessary for the three resource allocation schemes.

	Mode 2	Device sequential	Group scheduling
Discovery message (DM) content	• UE ID • Position & heading	• UE ID • Position & heading • Trigger time	• UE ID • Position & heading • Trigger time(s) • Leader selection • Sensed resource occupation (R_s) • Special forward indication
Resource selection message (RM) content	-	• Resources allocated by UE (A)	• Resources allocated to group members (A)
Data message	• Message periodicity • Application data	• Message periodicity • Application data	• Message periodicity • Application data

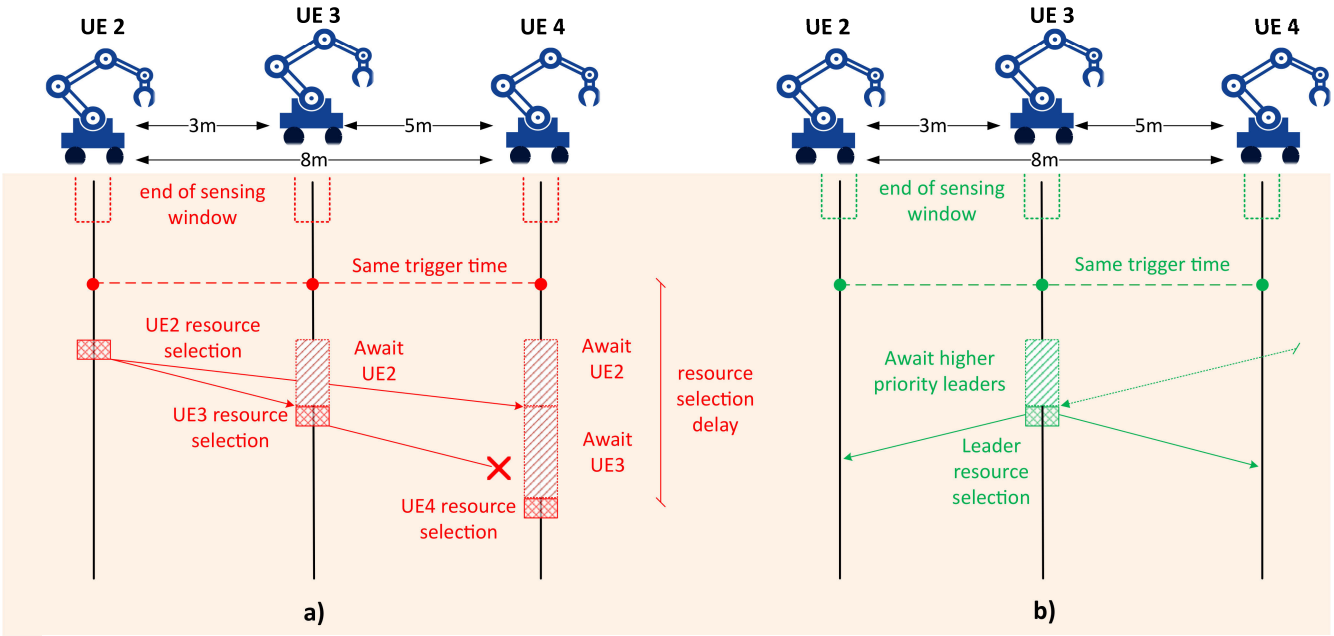

FIGURE 5. Control signaling exchange for (a) device sequential and (b) group scheduling.

once the resource selection delay expires (e.g., resource selection delay expires for UE 4 and it performs its resource allocation as illustrated in Fig. 5 (a)).

2) GROUP SCHEDULING

RMs are transmitted from the group leaders to their respective group members at the trigger time. If two or more leaders within r_e have group members with the same trigger time (e.g. the leader, UE 3, waits for higher priority leaders resource allocation in Fig. 5 (b)), they must follow the sequential procedure explained in Section IV-B1. In cases where multiple group members have been given resources simultaneously (e.g. UEs 2, 3, and 4 in Fig. 5 (b)), the group leader combines the selected resources in one RM. This is beneficial in dense scenarios, since it reduces the load of control signals in the control resource pool in comparison to the device sequential scheme. For the special forwarding procedure necessary in the edge case, group member UEs should forward the RMs (e.g. UEs 5 and 7 in Fig. 2 (b)) between leaders to enable leader-cooperation and hence, avoid half-duplex problems when allocating resources within their respective groups. The delay to perform resource allocation in the group scheduling scheme, scales with the number of leaders within r_e of each other. In addition, the special forwarding procedure introduces the delay of two additional transmission times. However, initiation of the resource allocation is bound by the configurable resource selection delay.

V. SYSTEM LEVEL EVALUATION

We consider an application for collective environment perception, in which robots within a proximity of $r_c = 5$ m must establish real-time high-throughput communication at high reliability for cooperative behavior, e.g. collision avoidance among robots and with external objects. This scenario is not unlike collective perception and cooperative collision avoidance from vehicle to anything (V2X) envisioned by 3GPP in [35]. Specific requirements for this scenario are a 10 Mbps throughput where message latency does not exceed 10 ms at a reliability of 99.99 % [35].

The robots are driving in a rectangular indoor factory building. Each robot moves according to the random waypoint mobility model, in which the robot moves at a fixed speed between random points within the factory. The 3GPP non-line of sight indoor factory, with sparse clutter and low base station (InF-SL) pathloss model from [36], is used for modeling the link pathloss. UE antennas are omnidirectional. As multiple links are in use, we impose correlation on the shadowing component. The shadowing is computed according to the method in [37], via integration over a Gaussian random field, using a 20 m de-correlation distance and 5.7 dB standard deviation. Fast fading is not explicitly modeled, but included in the link layer model. A new Gaussian random field and new starting positions of the UEs are applied each 200 seconds of the 1000 seconds simulation time. All comparisons, between swarm sizes and between schemes and techniques, use the same random field realizations.

Regarding 5G NR parameters we select numerology 2, dictating a $d_s = 0.25$ ms slot duration. The data channel bandwidth is 100 MHz, whereas the control data is carried on the smallest configurable sidelink sub-channel of twelve sub-carriers, resulting in a 7.2 MHz bandwidth. The lowest modulation and coding scheme (MCS) for sidelink has modulation order 2 and code rate $\frac{120}{1024}$, leaving at most 196 bits for the control messages. The MCS for the data transmission is dynamically adapted at the time of allocation. For each robot within r_c, the signal to interference and noise ratio (SINR) is calculated for the most recent transmission. The worst SINR is used to determine the modulation and coding scheme, from [38, Table 5.1.3.1-2], which can attain a 0.01 % target block error rate (BLER). The link level, hence the mapping from SINR to BLER, is modelled using a set of BLER curves generated from separate link level simulations [30]. The link level simulation includes all physical layer processing according to 5G NR. The required number of slots n_s are calculated based on the selected MCS, assuming that the transport block is bit padded to an integer number of slots. We do not differentiate between data message and control signal transmission in the link level modeling, which makes the control link performance slightly optimistic due to the much lower transmission bandwidth, i.e. 100 MHz compared to 7.2 MHz. The simulations parameters are listed in Table 3.

A. KEY PERFORMANCE INDICATORS

The main key performance indicator is reliability - the probability that a data message is received within the latency constraint. We measure it in the form of failure probability, equivalating a target 99.99 % reliability to a 10^{-4} failure probability. The failure probability pertains to each data message which is either received or not received. Under the assumption that the failure of each data message is independent and identically distributed, the failure probability has a binomial distribution. The simulation of data message receptions follows a Binomial distribution, with the number of trials being the number of attempted data message receptions and the number of successes describing the number of failed receptions of data messages. The failure probability is estimated accordingly, and the confidence intervals for the failure probability can be calculated using the Binomial or its large-sample Normal approximation, however, the actual coverage probability of such an (standard) interval is poor for probabilities near 0 or 1 according to [39]. Based on the conclusions of [39], we have calculated 95 % confidence intervals using both the Normal approximation and the Jeffreys confidence interval [39]. As an example, if we consider the curve for device sequential with signaling plus non-overlapping (red dotted curve) in Fig. 10 the 95 % Jeffreys confidence intervals on swarm size of 20 range from $2.1 \cdot 10^{-4}$ to $1.4 \cdot 10^{-4}$. In practice, it is difficult to assess the validity of the i.i.d. assumption. The assumption is weakened by the semi persistence of the resource selection and the relative slow change in simulated propagation environment. Given that the confidence intervals are small we have some confidence in comparing results across schemes and techniques.

As a complementary key performance indicator we capture the packet inter-reception (PIR) metric defined by 3GPP in [40]. It indicates the time in between successive packet receptions and is important for applications where regular updates are required.

Multiple reasons might cause a reception failure, e.g. half-duplex errors which arise when a UE is transmitting and therefore not able to receive a data message. We differentiate between whether a UE is transmitting a data message (half-duplex data), a discovery message (half-duplex DM), or a resource selection message (half-duplex RM). Interference is another source of data reception failure. We differentiate between interference caused by UEs within r_c, denoted *inner* interference, and interference by UEs outside r_c, denoted *outer* interference. When UEs within and outside r_c simultaneously cause interference we denote it as *mixed* interference. Lastly, when a group member has not received the resource selection message from its leader (no RM reception), it cannot perform a data message transmission which will cause data reception failures at the receivers.

VI. SIMULATION RESULTS

The control signaling exchange has a direct impact on the data message performance. It is fundamental to fulfill two conditions: first, the random selection of DM transmission must not coincide with the reception of data messages since it will cause half-duplex errors (half-duplex DMs); second, RMs failure probability should be sufficiently low such that it does not inhibit the performance of the cooperative schemes.

A. RELIABILITY ANALYSIS AND ENHANCEMENT TECHNIQUES

In Fig. 6 we present the failure probability and the causes at various swarm sizes for the three resource allocation schemes group scheduling (GSch), mode 2 (SLm2), and

TABLE 3. Simulation parameters.

Parameter	Value/range
Carrier frequency, f_c	3.5 GHz
Swarm size (number of UEs)	$[10, 20, 30, 40, 50, 60, 70]$
Critical cooperation range, r_c	5 m
Extended Cooperation range, r_e	25 m
Facility dimensions	120×50 m^2 [36]
Transmission power, P_{tx}	0 dBm
Data channel bandwidth	100 MHz
Control channel bandwidth	7.2 MHz
Resource selection delay	1.25 ms
NR slot duration	250 μs
Thermal noise power spectral density	-174 dBm/Hz
Receiver noise figure	9 dB
Interference	Independent intra-system
UE speed	1 m/s
Mobility model	Random waypoint (RWP)
Pathloss model	InF-SL [36]
Propagation condition	Non line of sight
De-correlation distance δ	20 m [37]
Discovery message periodicity	100 ms
Data message periodicity, d_p	10 ms
Data message size, x_d	100 kb
Data message latency requirement, l	10 ms
Simulation time	1000 s

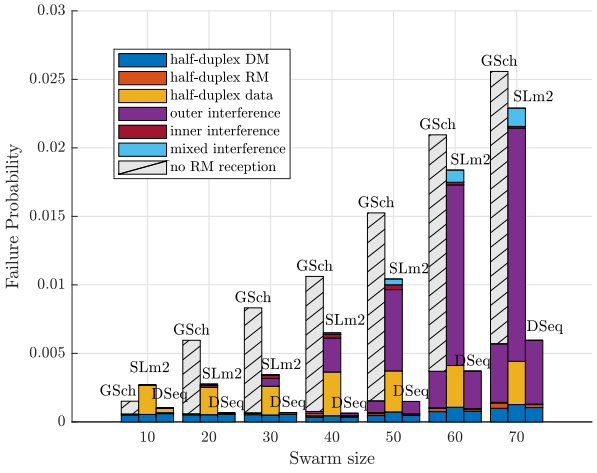

FIGURE 6. Failure probability and the causes of data transmission failures (half-duplex of DM, RM and data, inner, outer and mixed interference, and no RM reception) for three resource allocation schemes (SLm2, DSeq and GSch).

device sequential (DSeq). The data message failures fall in two general categories; those caused by half duplex and those caused by interference. The group scheduling scheme experiences failures from a third category related to failed reception of resource allocation messages (no RM reception). Even without the improvement techniques enabled, the device sequential RA scheme outperforms mode 2 in terms of failures caused by half duplex and interference. At small swarm sizes the main difference lies in mode 2 having a considerable number of half-duplex data failures. The half-duplex failures caused by transmission of RMs in the cooperative schemes constitute a minor performance impact. As swarm size increases, interference becomes a dominant failure cause. The lack of cooperation and the resource selection procedure of mode 2 (described in II-A2), result

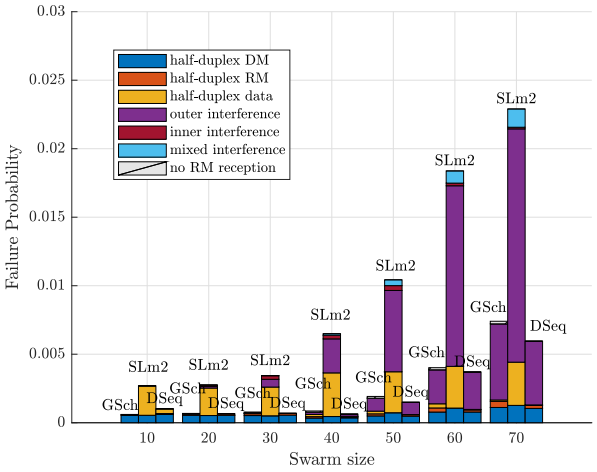

FIGURE 7. Failure probability and the causes of data transmission failures for three resource allocation schemes after enabling RM re-transmissions.

in UEs experiencing data reception failures caused by high interference coming from UEs outside cooperation range (outer interference), UEs inside cooperation range (inner interference), or both (mixed interference).

Failure to receive RMs in the cooperative resource allocation schemes can result in non-cooperative resource allocation. In the group scheduling scheme, a group member UE is dependent on receiving the RM from its leader. Failure of this RM reception (no RM reception) will result in failure to transmit data messages for the entire SPS data transmission period (grey hatched bars in Fig. 6). To address this issue the *RM re-transmission* technique was incorporated. It enables the group member to send a non-acknowledgment (NACK) to its leader, indicating that re-transmission of the RM is necessary. It might take several NACKs for a successful reception of RM. Fig. 7 illustrates how failures caused by no RM receptions diminish considerably.

The second largest failure cause (at small swarm sizes) is half-duplex failures caused by transmission of discovery messages (blue bars in Fig. 6). The random transmission of DMs has a significant impact on total failure probability of the cooperative resource allocation schemes. Mode 2 is similarly affected by the half-duplex DM. To counteract this problem we propose the *non-overlapping* technique. It utilizes the information about the current SPS transmissions acquired by UEs during the sensing procedure. The SPS transmission slots, acquired by other UEs, are not considered as possible options for the transmission of DMs to reduce potential half-duplex problems. Fig. 8 depicts the near disappearance of half-duplex DM failures.

A few half-duplex problems occur in receiving data messages due to simultaneous data message transmission (yellow bars in Fig. 6) for the cooperative schemes even at small swarm sizes. This indicates for the group scheduling scheme that leaders were not cooperating and for the device sequential scheme that some UEs failed to follow the sequential procedure. These described issues lead to the application

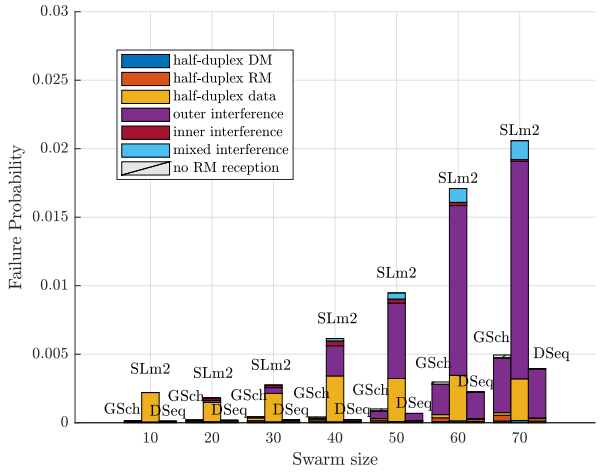

FIGURE 8. Failure probability and the causes of data transmission failures for three resource allocation schemes after enabling RM re-transmissions and non-overlapping techniques.

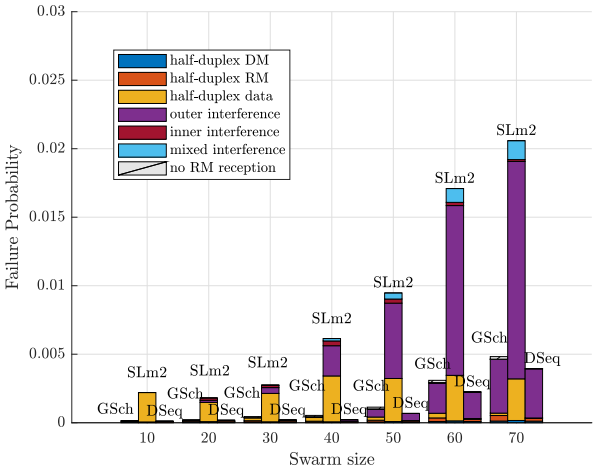

FIGURE 9. Failure probability and the causes of data transmission failures for three resource allocation schemes after enabling RM re-transmissions, non-overlapping and piggybacking techniques.

of the *piggybacking* technique for the respective resource allocation schemes. Piggybacking builds on repeating the resource selection information by appending it to other RMs. It is carried out as follows in the two cooperative schemes:

- *Device sequential:* When a UE receives RMs from its predecessors, it includes this information in its respective RM, so if UEs that follow the sequence did not receive previous RMs, they are able to recover them.
- *Group scheduling:* When the group leader sends an RM to a group member UE, it includes the information of prior transmitted RMs. It allows group member UEs an additional chance to receive its resource allocation when the leader schedules other group members.

Fig. 9 illustrates that, however, the effect of the piggybacking is negligible. This is a sign that the allocation sequences are not long enough, even at swarm sizes of 70 UEs, for the piggybacking technique to have an effect. Therefore, the piggybacking technique will not be included in the remaining evaluations.

At large swarm sizes, outer interference becomes the main cause of failure (we plan to address it in our future work).

B. RELIABILITY PERFORMANCE WITH ENHANCEMENTS

Fig. 10 shows the failure probability for different swarm sizes in simulations with the following configurations:

1) **Error-free signaling** in which every control message is received at every intended receiver.
2) **Error-prone signaling** according to the prevailing signal conditions.
3) **Signaling plus the RM re-transmission technique** in which in addition to 2) the RM re-transmission technique is utilized in the group scheduling scheme to mitigate data failures caused by failure to receive RMs.
4) **Signaling plus the RM re-transmission and the non-overlapping technique** in which in addition to 3) the non-overlapping technique is utilized to schedule DMs in time slots where no incoming data messages are expected.

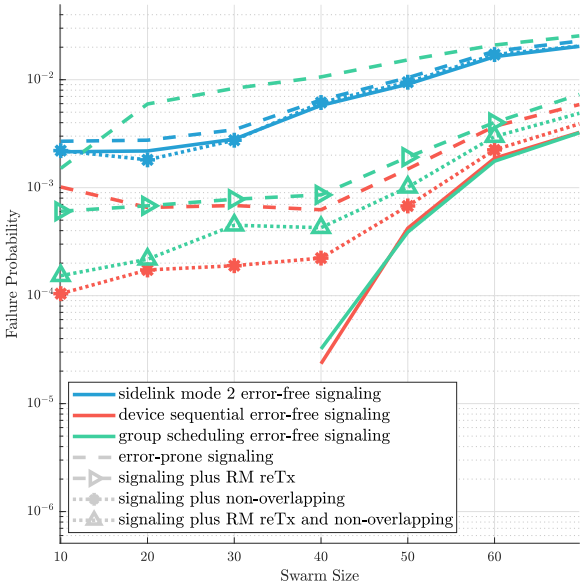

FIGURE 10. Failure probability for the resource allocation schemes at the five simulation configurations: error-free signaling, error-prone signaling, error-prone signaling with re-transmissions (only for group scheduling scheme), and error prone with non-overlapping (re-transmissions).

Mode 2 (blue lines in Fig. 10) reaches failure probability below 10^{-2} until a swarm size of 50. The failure probability of mode 2 is barely affected by the simulation configuration. The highest failure probability is observed in the error prone signaling configuration, where in addition to half-duplex data and interference, errors were caused by half-duplex DM. Enabling the non-overlapping technique brings the error probability of mode 2 down to the level of error free control signaling.

Device sequential resource allocation (red lines in Fig. 10) is affected by the enhancement techniques. With error prone signaling the failure probability can be maintained below 10^{-3} until a swarm size of 40. Enabling the non-overlapping

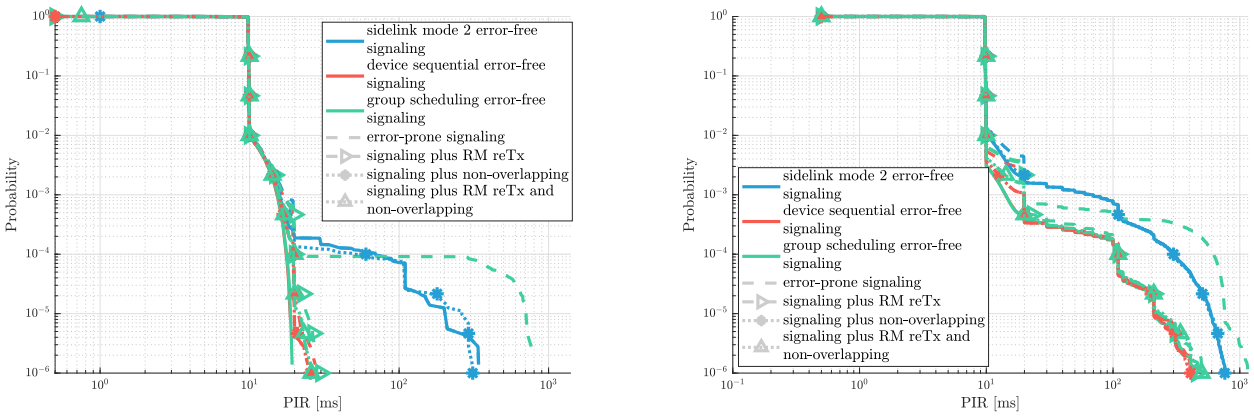

FIGURE 11. Packet inter reception (PIR) at swarm sizes of 20 UEs (a) and 70 UEs (b) for all simulation configurations.

technique further reduces the failure probability and allows it to maintain failure probability below 10^{-3} until swarm size of 50. With error-free signaling, the device sequential scheme experiences no failures at swarm sizes smaller than 40 UEs.

Group scheduling with error prone signaling has the highest failure probability of all schemes and configurations due to the impact on non-received RMs. However, enabling RM re-transmissions reduces the failure probability by an order of magnitude, and makes the performance comparable to the device sequential scheme in the error prone signaling configuration. Enabling non-overlapping further reduces the failure probability of the group scheduling scheme maintaining the failure probability below 10^{-3} until a swarm size of 50. With the evaluated enhancement techniques enabled the failure probability of group scheduling is still slightly higher than that of device sequential. With error free signaling, the group scheduling performance is as good as device sequential.

At swarm sizes 10 and 20 the failure probability of device sequential and group scheduling is not statistically different at the 0.05 significance level, cf. Jeffrey's confidence interval as discussed in Section V-A. At larger swarm sizes, device sequential obtains statistically significantly lower failure probability than groups scheduling for all the error-prone simulation configurations. In the error-free simulation configuration the device sequential and group scheduling has similar failure probability. This indicates that the device sequential signaling scheme is more efficient, even at larger swarm sizes.

C. PACKET INTER RECEPTION (PIR)

Fig. 11 (a) and (b) show the complementary cdf of the PIR for respectively 20 and 70 UE swarm size simulations. At both loads a PIR less than or equal to 10 ms is achieved on 99 % of data messages. This is expected, as the SPS period is exactly 10 ms, thus successive successful receptions of data messages in the same series of SPS transmissions will result in a 10 ms PIR. A PIR lower than 10 ms can occur as a result of re-selection of SPS transmission, and the same goes for PIR between 10 and 20 ms. However, PIRs longer than 20 ms are caused by reception failures. The configuration with the highest failure probability also experiences the most tailed PIR, regardless of the allocation scheme. At swarm size of 20, the PIR exceeds 20 ms with a probability less than 10^{-3}. Only mode 2 and the group scheduling configuration with error prone signaling experience 30 ms and above, corresponding to two successive reception failures. At swarm size of 70, all configurations experience PIRs greater than hundreds of milliseconds. The cooperative schemes perform similarly in configurations with RM-retransmissions enabled and outperform mode 2 at both swarm sizes.

VII. CONCLUSION

In this paper, we have extended our two previously proposed distributed cooperative resource allocation schemes - device sequential and group scheduling - with the required signaling support and have shown by a series of comprehensive system level simulations that the performance advantage of the cooperative schemes remains when signaling errors are considered. We have analyzed this in a detailed and accurate comparison to the NR sidelink mode 2 baseline, concluding that despite the increased susceptibility to signaling errors in the cooperative schemes, as a result of increased signaling overhead, the two cooperative schemes still have an order of magnitude reduction in failure probability compared to mode 2, hence much better reliability in delivering data messages successfully within a given latency constraint.

The methodology of identifying distinct causes of data failure provided valuable insight. Three enhancement techniques, respectively, resource selection message re-transmissions, non-overlapping allocation of discovery messages, and piggybacking, were designed to address the data transmission failures caused by the error prone control signaling. Resource selection message re-transmission and non-overlapping allocation of discovery messages proved to significantly reduce failure probability in the coordinated

schemes, whereas piggybacking did not introduce any significant gain.

The proposed resource allocation schemes, their associated control signaling, and enhancement techniques provide a good trade-off between control overhead and performance in terms of latency and reliability. However, in order to achieve the stringent 99.99 % reliability requirement additional interference management techniques are necessary. In our future work we will explore techniques to improve the reliability at larger swarm sizes.

REFERENCES

[1] I. Rodriguez, R. S. Mogensen, A. Schjørring, M. Razzaghpour, R. Maldonado, G. Berardinelli, R. Adeogun, P. H. Christensen, P. Mogensen, O. Madsen, C. Møller, G. Pocovi, T. Kolding, C. Rosa, B. Jørgensen, and S. Barbera, "5G swarm production: Advanced industrial manufacturing concepts enabled by wireless automation," *IEEE Commun. Mag.*, vol. 59, no. 1, pp. 48–54, Jan. 2021. [Online]. Available: https://ieeexplore.ieee.org/document/9356516/

[2] R. Arnold, J. Jablonski, B. Abruzzo, and E. Mezzacappa, "Heterogeneous UAV multi-role swarming behaviors for search and rescue," in *Proc. IEEE Conf. Cognit. Comput. Aspects Situation Manage. (CogSIMA)*, Aug. 2020, pp. 122–128.

[3] D. Albani, J. IJsselmuiden, R. Haken, and V. Trianni, "Monitoring and mapping with robot swarms for agricultural applications," in *Proc. 14th IEEE Int. Conf. Adv. Video Signal Based Surveill. (AVSS)*, Aug. 2017, pp. 1–6.

[4] A. R. Jordehi, "Optimal scheduling of home appliances in home energy management systems using grey wolf optimisation (Gwo) algorithm," in *Proc. IEEE Milan PowerTech*, Jun. 2019, pp. 1–6.

[5] S. Malik, K. Lee, and D. Kim, "Optimal control based on scheduling for comfortable smart home environment," *IEEE Access*, vol. 8, pp. 218245–218256, 2020.

[6] W. H. C. Wickramaarachchi, M. A. P. Chamikara, and R. A. C. H. Ratnayake, "Towards implementing efficient autonomous vacuum cleaning systems," in *Proc. IEEE Int. Conf. Ind. Inf. Syst. (ICIIS)*, Dec. 2017, pp. 1–6.

[7] S. Hegde, O. Blume, R. Shrivastava, and H. Bakker, "Enhanced resource scheduling for platooning in 5G V2X systems," in *Proc. IEEE 2nd 5G World Forum (5GWF)*, Sep. 2019, pp. 108–113.

[8] Q. Wu, S. Zhou, C. Pan, G. Tan, Z. Zhang, and J. Zhan, "Performance analysis of cooperative intersection collision avoidance with C-V2X communications," in *Proc. IEEE 20th Int. Conf. Commun. Technol. (ICCT)*, Oct. 2020, pp. 757–762.

[9] *Mesh Profile Rev. v1.0.1*, Mesh Working Group, San Jose, CA, USA, Jan. 2019.

[10] *IEEE Standard for Low-Rate Wireless Networks*, Standard 802.15.4-2020 (Revision IEEE Std 802.15.4-2015), 2020, pp. 1–800.

[11] *ERC Recommendation 70–03 Relating to the Use of Short Range Devices (SRD)*, CEPT, Tromsø, Norway, Feb. 2021. [Online]. Available: https://docdb.cept.org/download/25c41779-cd6e/Rec7003e.pdf

[12] *Electromagnetic Compatibility and Radio Spectrum Matters (ERM); Short Range Devices (SRD); Radio Equipment to be Used in the 25 MHz to 1 000 MHz Frequency Range With Power Levels Ranging up to 500 mW; Part 1: Technical Characteristics and Test Methods*, Standard ETSI EN 302 208-1, 2012.

[13] S.-Y. Lien, C.-C. Chien, F.-M. Tseng, and T.-C. Ho, "3GPP device-to-device communications for beyond 4G cellular networks," *IEEE Commun. Mag.*, vol. 54, no. 3, pp. 29–35, Mar. 2016.

[14] K. Mun, "CBRS: New shared spectrum enables flexible indoor and outdoor mobile solutions and new business models," OnGo Alliance (Former CBRSA Alliance), Sunnyvale, CA, USA, White Paper, 2017. [Online]. Available: https://www.everythingrf.com/whitepapers/details/3103-cbrs-ongo-new-shared-spectrum-enables-flexible-indoor-and-outdoor-mobile-solutions-and-new-business-models

[15] *Feature Lead Summary for AI 8.11.1.2 Inter-UE Coordination for Mode 2 Enhancements*, document RAN WG1#105-e Elections, 3rd Generation Partnership Project (3GPP), May 2021.

[16] Z. Yuan, Y. Ma, Y. Hu, and W. Li, "High-efficiency full-duplex V2V communication," in *Proc. 2nd 6G Wireless Summit (6G SUMMIT)*, Mar. 2020, pp. 1–5.

[17] A. Bazzi, C. Campolo, A. Molinaro, A. O. Berthet, B. M. Masini, and A. Zanella, "On wireless blind spots in the C-V2X sidelink," *IEEE Trans. Veh. Technol.*, vol. 69, no. 8, pp. 9239–9243, Aug. 2020. [Online]. Available: https://ieeexplore.ieee.org/document/9112708/

[18] S. Bartoletti, B. M. Masini, V. Martinez, I. Sarris, and A. Bazzi, "Impact of the generation interval on the performance of sidelink C-V2X autonomous mode," *IEEE Access*, vol. 9, pp. 35121–35135, 2021. [Online]. Available: https://ieeexplore.ieee.org/document/9361662/

[19] R. Molina-Masegosa, M. Sepulcre, J. Gozalvez, F. Berens, and V. Martinez, "Empirical models for the realistic generation of cooperative awareness messages in vehicular networks," *IEEE Trans. Veh. Technol.*, vol. 69, no. 5, pp. 5713–5717, May 2020. [Online]. Available: https://ieeexplore.ieee.org/document/9027961/

[20] H. Seo, J. Park, M. Bennis, and W. Choi, "Communication and consensus co-design for distributed, low-latency, and reliable wireless systems," *IEEE Internet Things J.*, vol. 8, no. 1, pp. 129–143, Jan. 2021.

[21] P. Di Lorenzo and S. Barbarossa, "Swarming algorithms for distributed radio resource allocation: A further step in the direction of an ever-deeper synergism between biological mathematical modeling and signal processing," *IEEE Signal Process. Mag.*, vol. 30, no. 3, pp. 144–154, May 2013.

[22] T. T. Doan and A. Olshevsky, "Distributed resource allocation on dynamic networks in quadratic time," *Syst. Control Lett.*, vol. 99, pp. 57–63, Jan. 2017.

[23] F. Peng, Z. Jiang, S. Zhang, and S. Xu, "Age of information optimized MAC in V2X sidelink via piggyback-based collaboration," 2020, *arXiv:2002.10242*.

[24] N. Bonjorn, F. Foukalas, F. Cañellas, and P. Pop, "Cooperative resource allocation and scheduling for 5G eV2X services," *IEEE Access*, vol. 7, pp. 58212–58220, 2019. [Online]. Available: https://ieeexplore.ieee.org/document/8613007/

[25] Y. Jeon, S. Kuk, and H. Kim, "Reducing message collisions in sensing-based semi-persistent scheduling (SPS) by using reselection lookaheads in cellular V2X," *Sensors*, vol. 18, no. 12, p. 4388, Dec. 2018. [Online]. Available: http://www.mdpi.com/1424-8220/18/12/4388

[26] S. Morejon, "Cooperative resource allocation in 6G proximity networks for robotic swarms," Ph.D. dissertation, Dept. Electron. Syst., Preben Mogensen, Aalborg Univ. Assistant Snr. Specialist Nuno Kiilerich Pratas, Nokia Standards Aalborg, Copenhagen, Denmark, 2022.

[27] *Physical Channels and Modulation*, Standard 3GPP TR 38.211 V16.0.0, 3rd Generation Partnership Project (3GPP), Dec. 2019.

[28] S.-Y. Lien, D.-J. Deng, C.-C. Lin, H.-L. Tsai, T. Chen, C. Guo, and S.-M. Cheng, "3GPP NR sidelink transmissions toward 5G V2X," *IEEE Access*, vol. 8, pp. 35368–35382, 2020. [Online]. Available: https://ieeexplore.ieee.org/document/8998153/

[29] J. Andrews, *Fundamentals of WiMAX: Understanding Broadband Wireless Networking*. Harlow, U.K.: Prentice-Hall, 2007.

[30] S. Lagen, K. Wanuga, H. Elkotby, S. Goyal, N. Patriciello, and L. Giupponi, "New radio physical layer abstraction for system-level simulations of 5G networks," in *Proc. IEEE Int. Conf. Commun. (ICC)*, Jun. 2020, pp. 1–7. [Online]. Available: https://ieeexplore.ieee.org/document/9149444/

[31] R. Zhang, X. Cheng, Q. Yao, C.-X. Wang, Y. Yang, and B. Jiao, "Interference graph-based resource-sharing schemes for vehicular networks," *IEEE Trans. Veh. Technol.*, vol. 62, no. 8, pp. 4028–4039, Oct. 2013.

[32] *Physical Layer Procedures for Data*, Standard TS 38.214 V16.4.0, 3rd Generation Partnership Project (3GPP), Dec. 2020.

[33] *Medium Access Control (MAC) Protocol Specification*, Standard TS 38.321 V16.5.0, 3rd Generation Partnership Project (3GPP), Dec. 2021.

[34] *5G; NR; Medium Access Control (MAC) Protocol Specification*, Standard TS 38.321 V16.5.0, 3rd Generation Partnership Project (3GPP), Jun. 2021.

[35] *5G; Service Requirements for Enhanced V2X Scenarios*, Standard TR 22.886 V16.2.0, 3rd Generation Partnership Project (3GPP), Dec. 2018.

[36] *Study on Channel Model for Frequencies From 0.5 to 100 GHz*, Standard 3GPP TR 38.901 V16.1.0, 3rd Generation Partnership Project (3GPP), Dec. 2019.

[37] S. Lu, J. May, and R. J. Haines, "Efficient modeling of correlated shadow fading in dense wireless multi-hop networks," in *Proc. IEEE Wireless Commun. Netw. Conf. (WCNC)*, Apr. 2014, pp. 311–316.

[38] *Physical Layer Procedures for Data*, Standard 3GPP TR 38.214 V16.0.0, 3rd Generation Partnership Project (3GPP), Dec. 2019.
[39] L. D. Brown, T. T. Cai, and A. DasGupta, "Interval estimation for a binomial proportion," *Stat. Sci.*, vol. 16, no. 2, pp. 101–133, May 2001. [Online]. Available: https://projecteuclid.org/journals/statistical-science/volume-16/issue-2/Interval-Estimation-for-a-Binomial-Proportion/10.1214/ss/1009213286.full
[40] *Study on Evaluation Methodology of New Vehicle-to-Everything (V2X) Use Cases for LTE and NR*, Standard TR 37.885 V15.3.0, 3GPP, Jun. 2019.

RASMUS LIBORIUS BRUUN received the B.Sc. degree in engineering (internet technologies and computer systems) and the M.Sc. degree in engineering (networks and distributed systems) from Aalborg University, Denmark, in 2015 and 2018, respectively. He is currently pursuing the Ph.D. degree with the Wireless Communication Networks Section, Aalborg University, in collaboration with Nokia Standardizations at the Aalborg, Denmark Office. His current research interests include mobile wireless ad-hoc networks, propagation modeling, and radio resource management.

C. SANTIAGO MOREJÓN GARCÍA received the B.Eng. degree in electronics and telecommunications from Escuela Politnica Nacional, Ecuador, in 2012, and the M.Sc. degree in mobile communications from Telecom ParisTech/Eurecom, France, in 2017. He is currently pursuing the Ph.D. degree with the Wireless Communication Networks Section, Aalborg University, in collaboration with Nokia Standardizations at the Aalborg, Denmark Office. His current research interests include radio resource management and interference mitigation for decentralized networks using 3GPP sidelink.

TROELS B. SØRENSEN received the M.Sc. degree in electrical engineering and the Ph.D. degree in wireless communications from Aalborg University, in 1990 and 2002, respectively. After the M.Sc. degree, he worked with type approval test methods as part of ETSI standardization activities. Since 1997, he has been with Aalborg University, where he is currently an Associate Professor with the Section for Wireless Communication Networks. He has successfully supervised more than 15 Ph.D. students and published more than 120 journals and conference papers. His current research interests include cellular network performance and evolution, radio resource management, propagation characterization, and related experimental activities.

NUNO K. PRATAS received the Licenciatura and M.Sc. degrees in electrical engineering from Instituto Superior Tecnico, Technical University of Lisbon, Lisbon, Portugal, in 2005 and 2007, respectively, and the Ph.D. degree in wireless communications from Aalborg University, Aalborg, Denmark, in 2012. He is currently a Senior Research Specialist with Nokia. His current research interests include wireless communications, networks, and the development of analysis tools for communication systems for 5G and 6G communications systems, in particular for sidelink use cases.

TATIANA KOZLOVA MADSEN received the Ph.D. degree in mathematics from Lomonosov Moscow State University, Russia, in 2000. Since 2001, she has been with the Department of Electronic Systems, Aalborg University, Denmark, where she is currently an Associate Professor of wireless networking. She has been involved in several national and international projects developing network architectures, network protocols, and solutions for intelligent transportation systems, smart grids, and automotive and train industries. Her current research interests include wireless networking, including quality of service and performance optimization of converging networks, communication protocols for the IoT systems and mesh networks, and methods and tools for performance evaluation of communication systems.

PREBEN MOGENSEN was a Full Professor with Aalborg University, in 2000, where he is currently leading the Wireless Communication Networks Section. He is also a Principal Scientist with the Standardization and Research Laboratory, Nokia Bell Labs. His current research interests include industrial use cases for 5G, 5G evolution, and 6G. He is a Bell Labs Fellow.